

Effects of Pb on SCC of Alloy 600 and Alloy 690 in Prototypical Steam Generator Chemistries

Jesse Lumsden^{1, a}, Allan McIlree^{2, b}, Richard Eaker^{3, c}, Rocky Thompson^{4, d}, and Steve Slosnerick^{5, e}

¹ Rockwell Scientific, 1049 Camino dos Rio, Thousand Oaks, CA, 91361, USA

² EPRI, 3412 Hillview Ave, Palo Alto, CA, 94304, USA

³ Duke Energy, 526 S Church Street, Charlotte, NC 28202, USA

⁴Florida Power Corp., 15760 West Power St., Crystal River, FL 34428, USA

⁵First Energy, 5501 N. State Route 2, Oak Harbor, OH 43449, USA

^a jlumsden@rwsc.com

^b amcilree@epri.com

^c reaker@duke-energy.com

^d rocky.Thompson@pgnmail.com

^e sslosnerick@firstenergycorp.com email

Keywords: Alloy 600, Alloy 690, Steam generators, Stress corrosion cracking, Intergranular corrosion, Corrosion potential, Lead cracking, Once through steam generators

ABSTRACT Intergranular attack/stress corrosion cracking of Alloy 600 continues to be an issue in the tube/tube support plate crevices and top of tubesheet locations of recirculating steam generators and in the upper bundle of free span superheated regions of once through steam generators (OTSG). Recent examinations of degraded pulled tubes from several plants suggest possible lead involvement in the degradation. Laboratory investigations have been performed to determine the factors influencing lead cracking in Alloy 600 and Alloy 690 steam generator tubes. The test environment is believed to be prototypical, with the addition of lead oxide, of a concentrated liquid phase existing in the pores of thin deposits on upper bundle tubes of an OTSG. Highly strained reverse U-bend specimens were tested at controlled electrochemical potentials. Maximum susceptibility was at open circuit potential, unlike cracking of Alloy 600 in caustic and acid sulfate environments where maximum susceptibility occurs when specimens are polarized above the open circuit potential. Transgranular, intergranular and mixed mode cracking was observed and in all Alloy 600 conditions tested (mill annealed, sensitized, thermally treated) while thermally treated Alloy 690 has so far resisted cracking. A film rupture/anodic dissolution model with displacement plating of Pb preceding passive film formation is consistent with the experimental observations

INTRODUCTION Intergranular attack/stress corrosion cracking (IGA/SCC) continues to result in steam generator tubing degradation and plugging of large numbers of tubes, and eventual replacement of steam generators. The main locations affected by IGA/SCC are the tube/tube support plate (T/TSP) crevices and top of tube sheet (TTS) locations in recirculating steam generators (RSGs), and in the upper bundle of the free span superheated regions of once through steam generators (OTSGs). The tube degradation in RSGs is caused by the concentration of impurities in T/TSP crevices. A thermohydraulic mechanism during the

generation of steam concentrates the impurities. In OTSGs, IGA/SCC is caused by liquid droplets in the superheated steam, which are transported to tube surfaces in the upper bundle, and where a more concentrated liquid phase forms in the pores of the deposits. Increases in water purity, and reductions in oxygen ingress have been generally successful in controlling most corrosion processes, but these measures have not prevented IGA/SCC. The present strategy for mitigating IGA/SCC is based on the premise that crack initiation and propagation rates depend on pH and the electrochemical potential. Accordingly, plants have adopted the practices of injecting hydrazine to maintain reducing conditions, and of adding amines to the feedwater to maintain the pH within the range of 5 and 9. These measures have been successful in reducing the rate of degradation in tubes affected by IGA/SCC in some plants; however, other plants using the same measures have continued to experience IGA/SCC. The reason for this variability is not well understood.

Pulled tube examinations performed over the years have implied that lead (Pb) may have been involved in numerous occurrences of IGA/SCC, but definitive evidence was many times lacking. Recently [3-6], high magnification analytical transmission electron microscopy (ATEM) has been used to examine degraded tube specimens and has revealed Pb within porous, nanocrystalline, degraded grain boundary oxides that were several nanometers wide. Other impurities found were Al, Si, Ca, K, and Mg. Although Pb is pervasive on the secondary side of steam generators, its involvement in IGA/SCC has generally been ignored because the concentration of Pb in deposits has been small in comparison to other contaminants. In the past, other causes of IGA/SCC, such as acid sulfate and caustic conditions, have been dominant, and Pb involvement, if any, has been considered a secondary cause. Staehle has recently produced a comprehensive review of the literature [7], and concluded that although there has been some progress in understanding PbSCC, there are important deficiencies in predicting and assuring steam generator life. This testing was undertaken to determine the factors influencing PbSCC in Alloy 600 and Alloy 690 steam generator tubes. The test environment is believed to be prototypical, with the addition of Pb, of a concentrated liquid phase existing in the pores of thin deposits on upper bundle tubes of an OTSG. The actual transport mechanism of Pb to the upper bundle region of an OTSG, i.e. Ocone [3], is not understood, and consequently for this study it is just assumed that the Pb exists in a concentrated liquid at some concentration.

EXPERIMENTAL

Tubing Material. Alloy 600 and Alloy 690 material was obtained as 15.9 mm diameter x 0.91 mm wall thickness steam generator tubing. The chemical composition of the alloys is given in Table 1.

Table 1

Chemical Composition of Alloy 600 and 690 Tubing Materials – wt. percent

ALLOY	C	Mn	Si	Cr	Ni	Al	Ti	Fe
600	0.05	0.22	0.34	16.3	75.2	0.19	0.17	7.54
690	0.02	0.42	0.29	29.9	58.7	0.09	0.19	10.3

The Alloy 600 tubing was received in a mill annealed (MA) condition, having a yield strength of 377 MPa (54.7 ksi) and a grain size of ASTM 9.5. The Alloy 690 tubing was received in a thermally treated (TT) condition, having a yield strength of 304 MPa (44.1 ksi) and a grain size of ASTM 6.6. The mill annealed Alloy 600 tubing was given either a thermal treatment (TT) (705°C for 15 hours) or a 'sensitizing treatment' (SN) (593°C for 18 hours) in a laboratory vacuum furnace. The degree of sensitization developed by these heat treatments was characterized by a 24 hour exposure in a modified Huey test, ASTM A262, using 25 w/o nitric acid. The weight loss for Alloy 600SN material was 1052 mg/dm²/day compared to 32 mg/dm²/day for 600TT and 15 mg/dm²/day for 600MA. Alloy 690TT had a weight loss of 3.0 mg/dm²/day in the Huey test. Material having a corrosion rate greater than 200 mg/dm²/day is generally considered sensitized.

Test Environments. Hideout return data and the results of OTSG pulled tube evaluations indicate that the concentrated liquid phase in the pores of the thin deposits on the upper bundle free span region has a complex chemistry composed of many species. The test environment(s) for this work was developed from analyses of hideout return data from several plants. Two environments were chosen; one simple and one complex. The simple environment contained 1.5 m Na₂SO₄ with a MULTEQ calculated pH at 330°C of 8. The complex environment, also contained 1.5 m Na₂SO₄, but in addition had 0.01 m Fe₃O₄ + 0.05 m Al₂O₃ + 0.3 m SiO₂ + 0.15 m KOH + 0.04 m HCL giving a MULTEQ calculated pH of 9. Both environments contained an initial hydrogen concentration of approximately 6 ppm, and were run with or without 50 or 500 ppm Pb added as PbO.

The solutions were prepared by first adding a calculated volume of demineralized (DI) water to the autoclave. Then the calculated weights of soluble components, NaCl, K₂SO₄, and KOH, were added and stirred until they dissolved. Weighed-out powders of SiO₂, Al₂O₃, Fe₃O₄, and PbO were mixed into the solution, but did not dissolve at room temperature. All tests were performed in Ti autoclaves, designed and constructed for the program. In each test, the quantity of electrolyte added was adjusted so that at test temperature, the electrolyte level was at least 5 mm above the top of the specimens. The cover gas was 5% hydrogen/95% argon. Before heating, the solution was deoxygenated in the autoclave by three pressurizing/aspirating cycles from 1.4 to 13.6 MPa (200 psia to 2000 psia). Each pressurization was held for 30 min followed by a slow release of the gas. No hydrazine was added for oxygen removal. Following the last aspiration, heating was begun with a 1.4 MPa (200 psia) overpressure to maintain a stable immersion level. The temperature of the autoclave was then brought up to the test temperature of 330°C. The final vapor pressure of the solution at the test temperature was approximately 14 MPa (2000 psia).

Potentiodynamic Polarization Curves. Potentiodynamic polarization tests were performed on the Alloy 600SEN and Alloy 690TT conditions in the simple environment. Tests were conducted in Ti autoclaves using the autoclave body as the counter electrode. The autoclave head had five symmetrically spaced openings for fittings to accommodate 3.2 mm diameter Ni or Alloy 600 rods, which were electrically isolated from the autoclave. One Ni rod was used as the reference electrode, where it was assumed that it was a hydrogen electrode. Although the Ni

reference rod may become coated with metal oxides, which precipitate from solution, the coatings are assumed to be porous and not electrochemically active; thus, the reference potential should have remained fixed by the hydrogen fugacity and pH. The remainder of the rods were used to suspend test specimens in the electrolyte. Potentiodynamic measurements were prepared by cutting “flag” specimens from the tubing. Each sample was a sector of the tubing one-fourth of the diameter and 12 mm wide with a 5cm x 3mm stem. The surfaces were polished to a final finish of 1 μm . The samples were spot welded to the ends of the alloy 600 rods and suspended so that the same area was exposed to the solution in all runs. The solution level was approximately mid-way up the stem. A Ni ring surrounded each specimen, and was used as the cathode. A Potentiostat/Interface connected to a PC was used to obtain the polarization curves. Curves were taken at a scan rate of 0.3 mV/s.

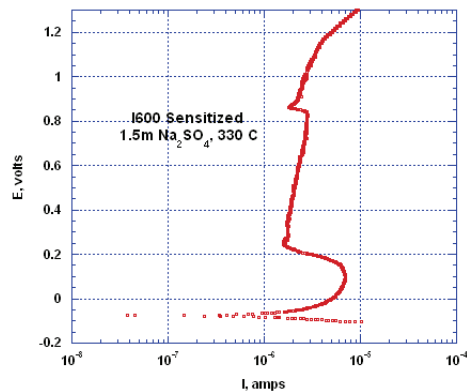
SCC Specimens and Tests. Reverse U-bend (RUB) specimens were fabricated by bending a 12.1 cm longitudinally split tube half over a 2.5 cm diameter mandrel with the inside diameter of the tube on the outside of the specimen in tension. After the deformed specimen was removed from the mandrel, the RUB was polished in the longitudinal direction using a Scotchbrite buffing wheel. The RUB was then re-strained by inserting an Alloy 600 bolt and nut through drilled holes at the base of the legs, and tightening until the legs were parallel.

The RUB specimens were configured in the Ti autoclaves. The ends of the screws used to apply stress to the RUB specimens were bolted to the Alloy 600 rods mounted on the autoclave head. Specimens were tested at open circuit or polarized potentiostatically using a potentiostat. Specimens were tested in the environment with and without 50 ppm Pb at 50 mV, 100 mV, and 150 mV above the open circuit potential. Specimens were also tested in an environment with 500 ppm Pb at open circuit, and at 50 mV above the open circuit potential. Test times were up to 4070 hours (24 weeks). Inspections were performed at various intervals ranging from a minimum of two weeks to as long as 8 weeks. After each exposure period, the specimens were examined for cracks using a low power optical microscope. After each inspection, all solids were removed from the autoclave, and it was brush cleaned and reloaded with fresh solution.

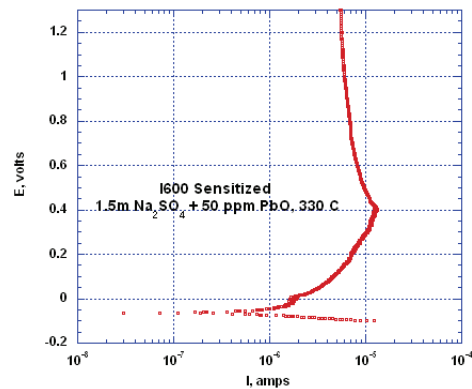
RESULTS

Potentiodynamic Polarization Curves

Figure 1 shows the polarization curves from sensitized Alloy 600 in the sulfate solution with and without Pb. This curve has an anodic peak which decreases rapidly and transitions into the passive region at approximately 250 mV. The jog in the curve at approximately 850 mV was due to an instrumental effect. The curve from the sensitized Alloy 600 specimen in the solution with Pb (Figure 1b) does not have an anodic peak, and has a current density several times higher at corresponding potentials. There were similar trends in the polarization curves from Alloy 690TT (Figure 2) except that there was not a pronounced anodic peak from the specimen in the solution without Pb.

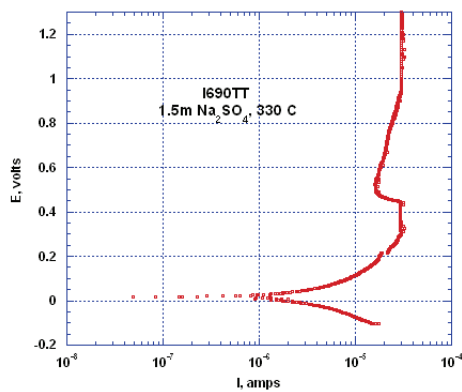


(a)

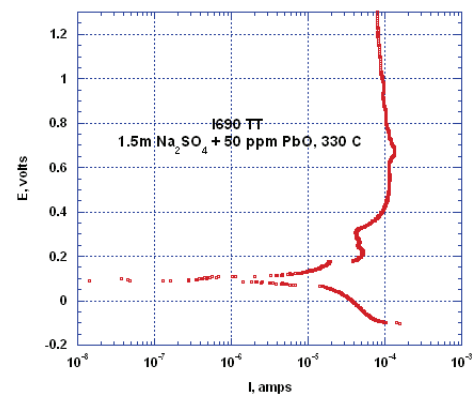


(b)

Figure 1. Polarization curves from sensitized Alloy 600 (a) in the solution without Pb and (b) in the solution with 50 ppm Pb.



(a)



(b)

Figure 2. Polarization curves from Alloy 690 in the solution (a) without Pb and (b) in the solution with 50 ppm Pb.

SCC Tests

Table 2 summarizes the RUB results for the four material conditions tested in the solution with 50 ppm Pb. The table also gives the results for Alloy 600SN and Alloy 600TT specimens polarized at 150 mV for 1340 hours in the test solution without Pb. For each potential, the table shows the exposure time, the number of specimens that cracked and the number tested. In some cases, the legs of the specimens were compressed (indicated by p for pinched) until the gap between them was decreased by 10% to 25%. Cracks were observed only in the two Alloy 600MA specimens polarized at 50 mV for 2000 hours. These cracks were not visible through a low power microscope until the legs of the specimens were compressed. A third Alloy 600MA

specimen was tested for 1800 hours while polarized at 50 mV, but no SCC was observed in this specimen. Two mill annealed specimens were also tested at 100 mV (one for 2000 hours and one for 3570 hours) and two specimens were tested at 150 mV for 2000 hours, but no SCC was observed. No SCC was observed in either of the two RUBs of Alloy 600SN, Alloy 600TT, and Alloy 690TT tested at 150 mV for 1340 hours. In addition, Alloy 600TT was tested at 50 mV and 100 mV for 1800 hours.

Table 2.

Results of destructive examination of RUB specimens in simple and complex environments after exposure to the test solution with or without (W/O) 50 ppm Pb.

Material/ECP	MA Alloy 600	SN Alloy 600	TT Alloy 600	TT Alloy 690
Complex W/O Pb;				
50 mV	No SCC of 2 after 2000 hrs			
100 mV	No SCC of 2 after 2000 hrs			
150 mV		No SCC of 2 after 1340 hrs		No SCC of 2 after 1340 hrs
Simple , 50 ppm Pb;				
OC, 0 mV		SCC 2 of 2 after 2400 hrs		No SCC of 2 after 3600 hrs
50 mV		No SCC of 2 after 3600 hrs		No SCC of 2 after 3600 hrs
100 mV		SCC 2 of 2 after 3600 hrs		No SCC of 2 after 3600 hrs
150 mV		No SCC of 2 after 3600 hrs		No SCC of 2 after 3600 hrs
Complex, 50 ppm Pb;				
50 mV	(a)SCC 2p of 2 after 2000 hrs, No SCC of 1 after 1800 hrs		No SCC of 2 after 1800 hrs	
100 mV	(a)No SCC 1p of 2 after 2000 hrs, No SCC of 1 after 3570 hrs		No SCC of 1 after 1800 hrs	
150 mV	(a)No SCC of 2 after 1340 hrs. No SCC 1p of 2 after 2000 hrs.	No SCC of 2 after 1340 hrs	No SCC of 2 after 1340 hrs	No SCC of 2 after 1340 hrs

The results for specimens tested in the complex environment with 500 ppm Pb are shown in Table 3. Two specimens of each material were tested at open circuit. In addition, two Alloy 600MA RUBs were tested at 50 mV. No SCC was observed after 4000 hours of exposure in the

Table 3**Summary of RUB SCC tests in complex environment with 500 ppm Pb**

Material/ECP	MA Alloy 600	SN Alloy 600	TT Alloy 600	TT Alloy 690
OC, 0 mV	SCC 2 of 2 after 840 hrs	SCC 2 of 2 after 1160 hrs.	SCC 2 of 2 after 2770 hrs.	No SCC of 2 after 4070 hrs.
50 mV	No SCC of 2 after 3150 hrs.	No SCC of 2 after 1650 hrs.	No SCC of 2 after 1650 hrs.	No SCC of 1 after 1650 hrs

RUBs polarized at 50 mV. Cracks were observed in both Alloy 600MA (after 840 hours), Alloy 600SN (after 1150 hours), and Alloy 600TT (after 2770 hours) in specimens tested at open circuit. It was not necessary to squeeze the legs of these specimens to reveal the cracks. The cracks in these specimens were clearly visible with the unaided eye. No SCC was detected in Alloy 690TT after 4070 hours of testing at open circuit.

Figure 3 is an optical micrograph of cracks in one of the Alloy 600MA RUBs that was tested at 50 mV in the solution with 50 ppm Pb. The specimen had dispersed intergranular cracks having a maximum penetration of approximately 250 μm . The penetrations are mostly single cracks with a few secondary cracks extending two or three grain boundaries beyond the main crack.

Metallography of the specimens tested in the 500 ppm Pb solution showed that the SCC morphology was different in each material. Figure 4 is a micrograph showing the crack paths in Alloy 600MA. Multiple deep penetrations are present. The maximum depth of the penetrations approaches 50% of the specimen thickness. Figure 4 shows that the cracks are intergranular, and that twin boundaries are also penetrated. Multiple cracks penetrating approximately 50% of the specimen thickness were also observed in Alloy 600SN (Figure 5). Unlike the intergranular cracks observed in Alloy 600MA, the cracks in Alloy 600SN were transgranular, and highly branched (Figure 5). There was mixed mode SCC in Alloy 600TT. Most cracks initiated as transgranular, and then became intergranular as cracks increased in depth (Figure 6). Alloy 600TT also had areas where volumetric IGA occurred. Areas of IGA were not observed in Alloy 600MA or Alloy 600SN.

An SEM examination showed that the cracks were filled with a corrosion product. An EDS analysis indicated that the corrosion product in the crack was the same as that on the surface which was a Ni, Cr silicate. A small amount of Pb was detected in the surface film. It was not conclusive that Pb was present in the EDS spectra from the corrosion products in the crack.

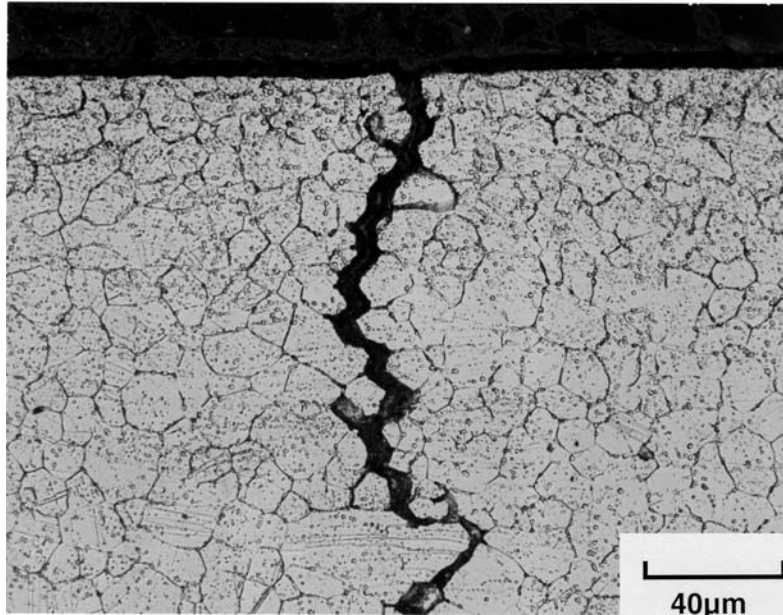


Figure 3. Micrograph showing IGSCC in the Alloy 600MA specimen that had been polarized at 50 mV in the solution with 50 ppm Pb, 500X.

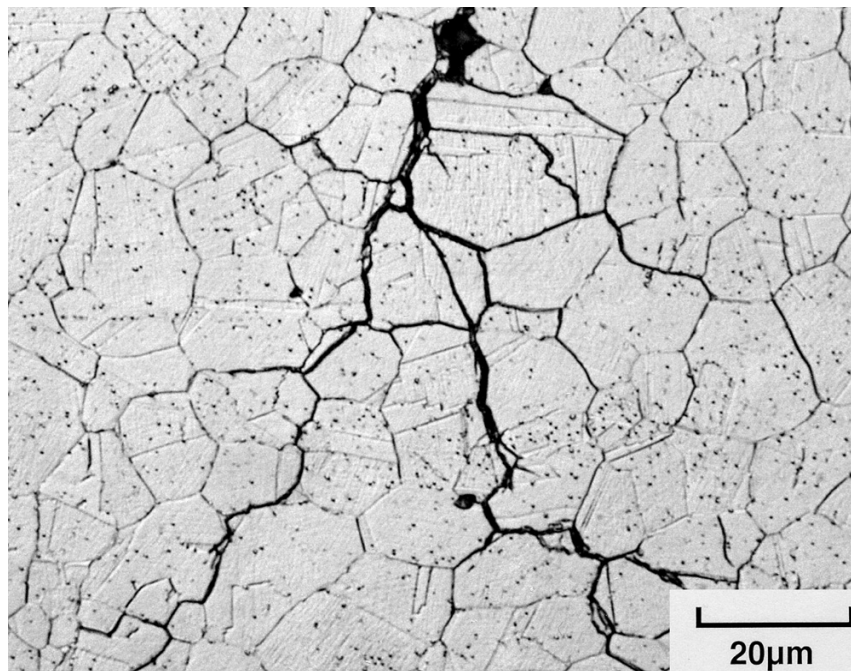


Figure 4. Micrograph showing IGSCC in the Alloy 600MA specimen that had been tested at open circuit in the solution with 500 ppm Pb, 1000X.

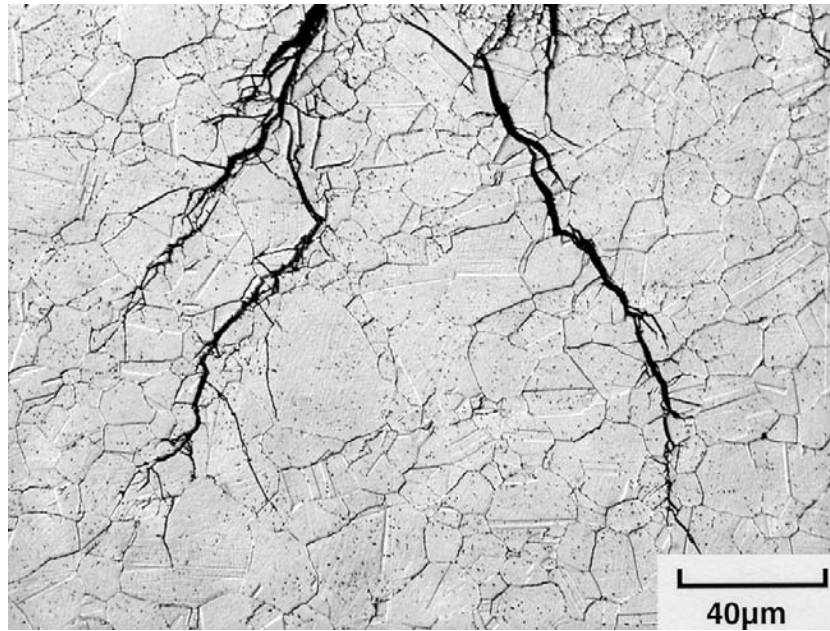


Figure 5. Micrograph showing IGSCC in the Alloy 600SN specimen that had been tested at open circuit in the solution with 500 ppm Pb, 500X.

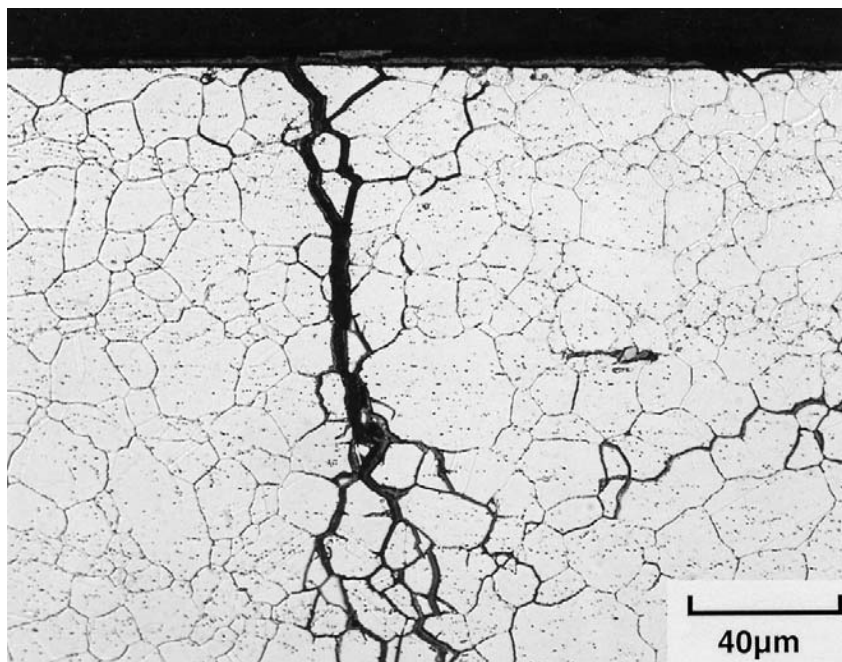


Figure 6. Micrograph showing IGSCC in the Alloy 600TT specimen that had been tested at open circuit in the solution with 500 ppm Pb, 500X.

The most severe cracking condition was open circuit. In a solution with 500 ppm Pb, PbSCC was observed in mill Alloy 600MA after 840 hours, in sensitized Alloy 600SN after 1150 hours, and in thermally treated Alloy 600TT after 2770 hours. No PbSCC was observed in thermally treated Alloy 690TT after 4070 hours. Cracking was not observed in the Alloy 600MA specimens polarized at 50 mV for 4000 hours. Tests were not performed at open circuit in the solution with 50 ppm Pb. But the most susceptible material in the 500 ppm Pb solution, Alloy 600MA, cracked after 1800 hours of exposure at 50 mV in the 50 ppm Pb solution; whereas, PbSCC was not observed in Alloy 600MA RUBs polarized at 100 mV and 150 mV after exposure for 3570 hours and 2000 hours, respectively.

DISCUSSION

There are two aspects of these PbSCC laboratory results for Alloy 600 that have not been observed in other, non-lead containing environments and other alloy/environment systems. The first difference is the potential dependence. In other environments [14-16], the most severe SCC conditions occurred at potentials anodic to the open circuit potential (oxidizing conditions) [4]. The second difference is the change in cracking mode with material condition. PbSCC in Alloy 600MA was intergranular, transgranular in Alloy 600SN, and mixed mode in Alloy 600TT. These results also show that transgranular cracking is not a definitive indication of PbSCC as sometimes believed.

Unlike SCC of Alloy 600 in high temperature caustic and acid sulfate solutions where maximum susceptibility is at highly oxidizing conditions, Alloy 600 is most susceptible to PbSCC at open circuit. An inspection of the Pourbaix diagrams for Ni and Pb offers an explanation for the potential dependence of PbSCC. Figure 7 (from Staehle [7]) shows the superposition of the Ni

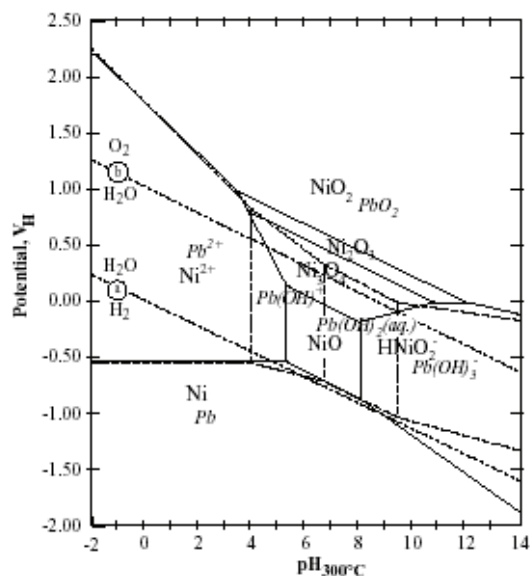


Figure 7. Superposition of Pourbaix diagrams for Ni (solid lines) and Pb (dotted lines) for 300°C.

and Pb Pourbaix diagrams at 300°C. Pb is soluble over the full range of pH's, assuming that the only soluble species present are Ni^{+2} , Pb^{+2} , and soluble hydroxides of Pb and Ni, except at very high oxidizing conditions where PbO_2 forms. However, Ni forms insoluble NiO in the mid-range of pHs and has zones at high and low pHs where soluble compounds are thermodynamically stable. Thus, the superimposed Pourbaix diagrams for Pb and Ni suggest that Pb will not exert an effect on the passivation behavior of Ni based alloys, as was found experimentally in polarization curves in Figures 1 and 2. In deoxygenated, high temperature, aqueous solutions, the corrosion kinetics of Alloy 600 and Alloy 690 are under cathodic control. Under these conditions, the open circuit (free corrosion potential) is typically near the reversible hydrogen potential for the test solution. The Pourbaix diagram in Figure 7 indicates that this is near the phase boundary between Ni/NiO and Pb/soluble Pb species. Thus, when the oxide film is ruptured by an emerging slip step, Pb begins to deposit on the new surface by displacement plating. In this process, alloy dissolution is the balancing anodic reaction. Since plating kinetics are faster than anodic oxidation, a Pb layer forms before the passive film can form. A layer formed by displacement plating is inherently porous. The pores are channels for transport of metal ions into the crack tip chemistry. The low concentration of Pb ions and high anodic current density through the pores lead to a thin Pb layer and rapid formation of the passive oxide. The oxide blocks the pores in the Pb and covers the surface. Without the Pb deposition step, repassivation by an oxide film is rapid and SCC does not occur. The formation of the Pb layer slows repassivation to the extent that a crack initiates and propagates.

The proposed mechanism for PbSCC is shown in Figure 8. This figure also shows schematically deposit build up in the on the freespan and the solution concentrating effects in the pores in the deposits

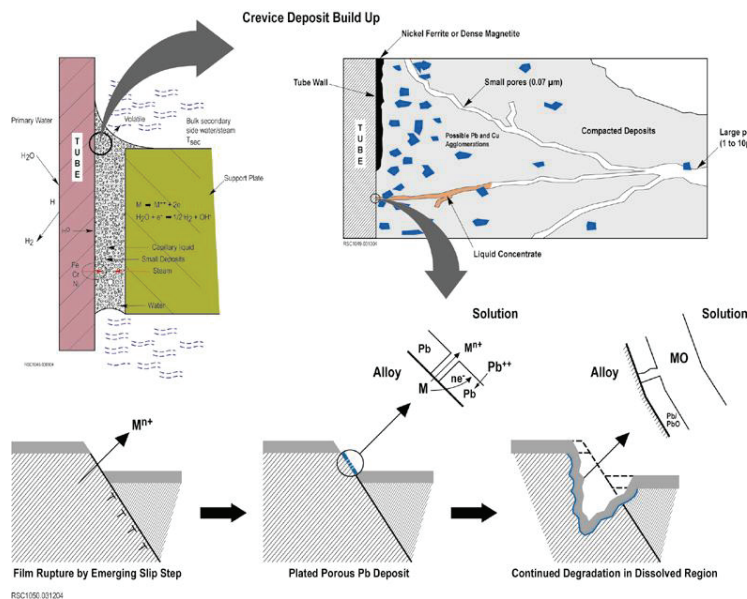


Figure 8. Proposed Mechanism of PbSCC .

This proposed mechanism is consistent with ATEM results [3-6] where Pb is found in a narrow ribbon at the alloy oxide film/alloy interface or included in the alloy oxide. Whether Pb exists as a ribbon or appears to be incorporated in the oxide depends upon the porosity of the deposited Pb. Porosity depends on the soluble Pb concentration, and species in the crack tip chemistry that interfere with the plating process. The existence of a plated Pb layer also offers a rationalization of the increased current density in the polarization curves for Alloy 600 and Alloy 690 (Figures 1 and 2) in the sulfate solution with Pb. The plated Pb is stripped by anodic dissolution as the applied potential moves into the region of the Pourbaix diagram where only soluble Pb species exist. The additional observation that the anodic current density for both test solutions is higher for Alloy 690 than Alloy 600 likely occurs because Alloy 690 has higher Cr than Alloy 600. Chromium is more soluble in alkaline solutions than Ni.

CONCLUSIONS

- Maximum PbSCC susceptibility in an environment containing 500 ppm Pb was observed at open circuit potential (OCP). This differs from Alloy 600 SCC in lead-free caustic and acid sulfate environments, where maximum susceptibility occurs when specimens are polarized above the OCP.
- Transgranular, intergranular, and mixed mode cracking were observed in all Alloy 600 conditions tested (mill-annealed, sensitized, and thermally treated), while thermally treated Alloy 690 has thus far resisted cracking.
- Relative to the Alloy 600 mill-annealed condition, the sensitized condition lasted 1.4 times longer, and the thermally treated condition lasted 3.3 times longer. Thermally treated Alloy 690 lasted at least 4.8 times longer.
- A Pb layer was found adjacent to the substrate on the crack walls and at the crack tip. A nickel-chromium-iron oxide film approximately 5 nm thick covered this layer.
- A mechanism involving displacement plating is consistent with the increased severity of PbSCC at open circuit and with the ATEM results.

ACKNOWLEDGEMENTS

The experimental portions of this work was funded by the EPRI Steam Generator Management Program, and the B&W Owners Group.

REFERENCES

- [1] P. A. Sherburne: *Surface Analysis of Oconee Unit 1 Steam Generator Tubes*, Proceedings: 1996 EPRI Surface Chemistry Workshop, TR-112481.
- [2] J. B. Lumsden: *Insights on Local Chemistry and IGA/SCC from Surface Analysis of Pulled Tubes*, Proceedings: 1996 EPRI Surface Chemistry Workshop, TR-112481.

- [3] D. P. Rochester and R. W. Eaker: *Laboratory Examination Results from Oconee Nuclear Station Once through Steam Generator Tubes*, 9th Environ. Degrad., TMS, 2000, p.639.
- [4] L. E. Thomas, V. Y. Gertsman and S. M. Bruemmer: *Crack-Tip Microstructures and Impurities in Stress-Corrosion-Cracked Alloy 600 from Recirculating and Once-Through Steam Generators*, 10th Environ. Degrad., NACE, 2002.
- [5] L. Thomas and S. Bruemmer: *Analytical Electron Microscopy of Intergranular Attack and Stress Corrosion Cracks in Alloy 600 Tubes Removed from Recirculating Steam Generators*, EPRI, Palo Alto, CA: 2003, 1003587.
- [6] L. Thomas and S. Bruemmer: *Analytical Electron Microscopy of Pulled Alloy 600 Steam Generator Tubes from Comanche Peak Unit 1 and Seabrook Unit 1*, EPRI, Palo Alto, CA: 2004, 1009346.
- [7] R. W. Staehle: *Assessment of and Proposal for a Mechanistic Interpretation of the SCC of High Nickel Alloys in Lead-Containing Environments*, 11th Environ. Degrad. ANS, 2003, p.381.
- [8] H. R. Copson and S. W. Dean: *Effect of Contaminants on Resistance to Stress Corrosion Cracking of Ni-Cr Alloy 600 in Pressurized Water*, Corrosion 21, 1 (1965).
- [9] G. P. Airey: *Effect of Carbon Content and Thermal treatment on the SCC Behavior of Inconel 600 Steam Generator Tubing*, Corrosion 35, 129 (1979).
- [10] G. O. Hayner, et al. : *Examination of Tubes Removed from St. Lucie Unit 1 and Investigation of Causes of the Corrosion*, 3rd Environ. Degrad., TMS, 1988, p 449.
- [11] A. Agrawal and J. P.N. Paine: *Lead Cracking in Alloy 600-A Review*, 3rd Environ. Degrad., NACE, 1990, p. 7-1.
- [12] B. P. Miglin and J. M. Sarver: *Investigation of Lead as a Cause of Stress Corrosion Cracking at Support Plate Intersections*, NP-7367, EPRI, Palo Alto, CA, 1991.
- [13] H. Takamatsu, et. al: *Study on Lead-induced Stress Corrosion Cracking of Steam Generator Tubing under AVT Water Chemistry Conditions*, 8th Environ. Degrad. of Materials in Nuclear Power Systems-Water Reactors, ANS, 1997, p. 216.
- [14] J. B. Lumsden and A. McIlree: *Effects of Alumino-Silicate on the Stress Corrosion Cracking of Alloys 600 and 690*, 11th Environ. Degrad., ANS, 2003, p.381.
- [15] D. van Rooyen: *Review of Stress Corrosion Cracking of Inconel 600*, Corrosion, 597, 31 (1975).
- [16] W. H. Cullen and M. J. Partridge: *Susceptibility of Alloys 600 and 690 to Acidified Sulfate and Chloride Environments*, EPRI, Palo Alto, CA, TR-104045, 1994.

- [17] M. Helie, I. Lambert, and G. Santarini: *Some Considerations about the Possible Mechanisms of Lead Assisted Stress Corrosion Cracking of Steam Generator Tubing*, 7th Environ. Degrad., NACE, 1995, p.247.
- [18] S. M. Bruemmer, and C. H. Henager Jr: *Microstructure, Microchemistry, and Microdeformation of Alloy 600 Tubing*, 2nd Environ. Degrad., ANS, 1985, p. 293.
- [19] S. M. Bruemmer.: *Interfacial Precipitation, Segregation and Deformation in Alloy 600: Implication on Primary-Side IGSCC*, EPRI TR-104898, December 1996